

***Ab initio* structural and electronic analysis of CH₃SH self-assembled on a Cu(110) substrate**

S. D'Agostino, L. Chiodo, F. Della Sala, R. Cingolani, and R. Rinaldi

National Nanotechnology Laboratory of CNR-INFN, c/o Distretto Tecnologico ISUFI, Università del Salento, via Arnesano, I-73100, Lecce, Italy

(Received 29 January 2007; published 31 May 2007)

Ab initio Density Functional Theory calculations are here reported to characterize the adsorption of methanethiol at the Cu(110) surface. Theoretical results suggest that the binding of the adsorbate to the substrate is rather weak and the molecular geometry is correspondingly almost unaffected by the adsorption. Otherwise, when CH₃SH deprotonates producing methanethiolate, a stronger chemical bond is realized between the sulfur atom of CH₃S radical and Cu surface atoms. A detailed study of structural and electronic properties of methanethiolate on Cu(110) for a $p(2 \times 2)$ and a $c(2 \times 2)$ overlayer structure has been carried out. We find that, in the most stable configuration, the molecule adsorbs in the shortbridge site. The chemical bond arises due to a strong hybridization among p orbitals of sulfur and d states from the substrate, as it is deduced by an analysis of partial densities of states and charge densities.

DOI: 10.1103/PhysRevB.75.195444

PACS number(s): 68.43.Bc, 68.43.Fg, 68.43.-h, 73.20.-r

I. INTRODUCTION

The adsorption of alkanethiol compounds on metal surfaces has been the focus of many studies in the last two decades.¹⁻³ The interaction of alkanethiols with surfaces is in fact of high interest in many applications such as functionalization of surfaces, wear protection, corrosion inhibition, lubrication, and chemical sensors fabrication.⁴⁻⁹ Moreover these species, through deprotonation at the interface, form thiolate self-assembled monolayers (SAMs) which are interesting as conductive channels in molecular electronics¹⁰ or as barrier films to retard oxidation of a metal surface.¹¹ The structural properties of self-assembled monolayers of thiols on metals, thanks to their highly ordered or atomically flat surfaces have been largely studied by scanning tunneling microscopy,¹²⁻¹⁸ electron diffraction,¹⁹ low energy helium diffraction,²⁰⁻²² grazing incidence x-ray diffraction^{14,22} and grazing incidence infrared spectroscopy.²³⁻²⁵

In addition, their highly ordered structures make these systems ideal for studies by *ab initio* computational methods.²⁶ The largest part of the theoretical studies concerns the adsorption of thiols,²⁷⁻³⁰ with different tails, on Au(111) surface, in particular CH₃S (Ref. 31) and (CH₃S)₂,³²⁻³⁵ long chain alkanethiols,³⁶ and cysteine.^{37,38} The structural description of such systems is not straightforward. The long-range superstructure is well established to have a hexagonal ($\sqrt{3} \times \sqrt{3}$)R30° symmetry, but the determination of the exact adsorption site for alkanethiols on Au(111) has been controversial: actually the most stable adsorption site should be the bridge site shifted towards the fcc hollow site,³² even in competition with the pure bridge site.³³ Most recent experimental results, supported by theoretical calculations,²⁹⁻³¹ report a new superstructure, which implies a reconstruction of the flat Au(111) with vacancies or adatoms, giving even most stable adsorption configurations.

In the structural analysis, apart from the adsorption site, the angle between the molecule and the normal to the surface must be included, strongly affecting the stability and the electronic properties of the interface. For more complex mol-

ecules, such as cysteine and thiophene, the molecular tail orientation can also modify the system properties.^{37,39} Most recent analyses are now focused on electronic properties of such interfaces, in particular the metal work function modifications induced by the SAMs.^{40,41}

In this framework, various experimental and theoretical studies related to adsorption and decomposition of CH₃SH on different (111) and (001) transition-metal surfaces have been carried out.^{32,42,43} The choice of using methanethiol, the simplest organic thiol, is due to its dimensions, which exclude large effects due to molecular chain orientation and allow to concentrate on the interface properties, which finally dominate the behavior of metal-molecule systems. In fact, it is well established that, even for large thiols, the interaction at the S-Au interface is due to the p -S/ sd -Au hybrid states.^{37,44}

The same happens at the S-Cu interfaces,⁴⁵⁻⁴⁷ which have been however less deeply investigated than Au, both experimentally and theoretically. Copper has retained for a long period an important role in the clarification of the electronic structure of solids. Experimentally, being an inert material easy to handle, it has been extensively studied: its energy dispersion relations, lifetimes of the band states, surface states have been determined with considerable precision.^{48,49} Moreover this metal could present very interesting properties useful to realize nanodevices: it has been observed, for example, that after adsorption and decomposition of particular macromolecules (such as C₉₀H₉₈) on a Cu surface it is possible to notice an important superficial reconstruction and also the creation of nanometrical islands of metal atoms: such kind of reconstructed steps can be used as a guidance for lateral manipulation of large molecules.⁵⁰

It is known that thiol molecules adsorb in square geometries on Cu(001) and Cu(111) surfaces, and that mainly the $p(2 \times 2)$ and $c(2 \times 2)$ superstructures are observed on these substrates.^{51,52} The (001) Cu face, due to its square symmetry,⁵³ results to be quite favorable for sulfur and thiols adsorption, with preferred fourfold hollow site adsorption. It is known, on the other side, that Cu(111) is less well suited,

also with respect to its Au analogous, for thiols ordered adsorption, due to the low energy difference between different adsorption sites.⁵⁴ The most stable site results to be the bridged one, and the long-chain thiols show a tilt angle of $\approx 50^\circ$ with the surface normal. In particular, on the hexagonal (111) surface, the adsorption of sulfur, or of species containing sulfur, induces a square surface reconstruction similar to the (001).⁵⁵

Here we are interested in the adsorption geometry and decomposition of methanethiol on the (110) copper surface, a system which presents experimental problems not yet completely solved.⁵⁶ The (110) case seems to be quite more complex, with respect to the other two high symmetry surfaces, because of the lower, rectangular symmetry of this face. In fact, the sulfur atoms deposition gives rise, depending on the coverage, to various reconstructions, experimentally observed by low-energy electron-diffraction (LEED),⁵⁷ and the adsorbate-induced strain yields surface corrugation and buckling.⁵⁷ The exact geometry of these large reconstructions has not yet been completely clarified. Therefore, we expect that also the adsorption geometry of thiol molecules through sulfur atoms could result to be more complex on the (110) surface³⁸ than on square symmetry surfaces.

It is experimentally known, from combined x-ray photoelectron spectroscopy (XPS), scanning tunneling microscopy (STM) and temperature programmed desorption (TPD) studies,⁵⁶ that the adsorption of methanethiol on the clean Cu(110) surface is characterized by the formation, through the S-H bond cleavage, of an adsorbed mercaptide and by an induced surface reconstruction with very narrow terraces (typically $10 \div 15 \text{ \AA}$ wide) oriented mainly in the $[\bar{1}10]$ direction: higher resolution images of the terraces, at molecular concentrations higher than $3 \times 10^{14} \text{ cm}^{-2}$ ($\approx 0.28 \text{ ML}$ coverage), reveal an atomic scale structure with a $c(2 \times 2)$ unit cell containing two mercaptide species. In the adsorption geometry, proposed according to measurements of time-of-flight electron-stimulated desorption ion angular distribution (TOF-ESDIAD) and to LEED images,⁵⁸ the methanethiolate is oriented on Cu(110) in a lying-down position, with a C-H bond quite close to the normal direction on average.

Few experimental studies are available for larger molecules adsorption on Cu(110). A long-chain thiol, the dodecanethiol, shows on Cu(110) a local $c(2 \times 2)$ structure, while the long-range order results in a complex $c(12 \times 16)$ unit cell. Tilt angles for n -thiols ($n=6 \div 16$) of $12^\circ \div 25^\circ$ have been observed.⁵⁹ L-cysteine, which also adsorbs through the sulfur atom, shows a $c(2 \times 2)$ structure on Cu(110).⁶⁰

In this paper we present Density Functional Theory (DFT)⁶¹ calculations of structural and electronic properties of CH_3SH on Cu(110): we find that, when the molecule is not deprotonated, the binding of the adsorbate to the substrate is rather weak, and that chemisorption occurs only when the molecule decomposes producing methanethiolate. We report a detailed study of the adsorption of mercaptide, analyzing the two coverages $\theta=0.25 \text{ ML}$ and $\theta=0.50 \text{ ML}$ for various configurations, and determining the most stable adsorption geometries and the corresponding strength of the adsorbate-substrate chemical bond. We confirm the stability of the $\theta=0.50 \text{ ML}$ coverage,⁵⁶ but we can exclude the flat-

lying orientation for methanethiolate,⁵⁸ finding an angle of $40^\circ \div 50^\circ$, depending on the adsorption geometry, of the molecular axis with respect to the normal to the surface. Through density of states (DOS) and spatial electronic charge distributions, moreover, it is possible to highlight the centrality of sulfur atoms in the binding process. For this reason these results can be considered relevant in the most general understanding of the self-assembly of alkanethiol layers on metal surfaces.

II. COMPUTATIONAL METHOD

Calculations presented in this paper have been performed in the framework of DFT using the Generalized Gradient Approximation (GGA) in the Perdew-Burke-Ernzerhof parametrization⁶² and, for some of the analyzed systems, in the Local Density Approximation (LDA).⁶³ All calculations for $\text{CH}_3\text{SH}/\text{Cu}(110)$ and $\text{CH}_3\text{S}/\text{Cu}(110)$ have been performed with the PWSCF code,⁶⁴ and all figures of the adsorption geometries and electronic charge densities have been realized by the XCRYSDEN graphical package.⁶⁵ Atoms are described by ultrasoft pseudopotentials,⁶⁶ with a kinetic energy cutoff of 35 Ryd: preliminary calculations on Cu bulk have demonstrated that this cutoff is sufficient to achieve convergence of 0.01 eV on the total energy and of 0.001 eV on the eigenvalues of the system. The cubic lattice constant a has been optimized minimizing total energy of the bulk Cu in both GGA and LDA approximations. Our GGA (LDA) calculations yield a lattice parameter of 3.67 \AA (3.51 \AA) which is quite close to the experimental value of 3.61 \AA ,⁶⁷ and in excellent agreement with the theoretical values obtained by Favot.⁶⁸ The Fermi energy has been calculated using the Gaussian broadening technique,⁶⁹ with a smearing parameter of 0.05 Ryd.

In hybrid systems different parts of adsorbate (head group, surface group, and chain) have, generally, different functions and roles in the formation of chemical bonds. In order to determine the atom or the group of atoms responsible for the formation of bonds in the $\text{CH}_3\text{SH}/\text{Cu}(110)$ system, a theoretical analysis of adsorption, both from a structural and also from an electronic point of view, has been made by adopting a supercell scheme. This analysis of structural properties has been performed in the framework of the GGA, which is able to give the most realistic values for bond lengths and binding energies for complex adsorbate systems.^{68,70} Three different kinds of systems are needed to study adsorption properties: the isolated molecules of methanethiol and dimethyl disulfide (CH_3S)₂, the clean copper surface, and the molecular-metal interface. The isolated molecules have been analyzed using a large vacuum box of 10 \AA side, to avoid spurious intermolecular interactions. The clean Cu(110) surface is modeled by a seven layers slab and 10 layers vacuum supercell,⁷¹ while, to study the molecule-substrate interaction, the supercell adopted in the present calculation has a 2×2 surface unit cell. The use of 10 vacuum layers, corresponding to a distance of $\approx 13 \text{ \AA}$ between two adjacent slabs, is necessary to reduce the interactions of surface states through the vacuum region, also in the presence of adsorbates. The 2×2 unit cell has basis vectors a_1 , a_2 ,

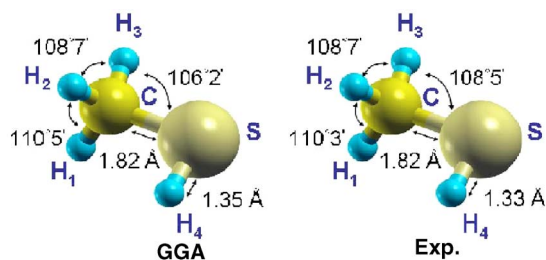


FIG. 1. (Color online) Methanethiol structural parameters, theoretical (left-hand picture) and experimental (Ref. 75) (right-hand picture) results.

and a_3 where a_1 and a_2 , on the (110) surface, are of length $2a/\sqrt{2}$ and $2a$, along the direction $[1\bar{1}0]$ (x) and $[001]$ (y), respectively, while a_3 , orthogonal to the (110) surface, is of length $16a/2\sqrt{2}$. The Brillouin-zone (BZ) integration is performed with a $8 \times 8 \times 1$ Monkhorst-Pack⁷² mesh, corresponding to 16 k -points in the irreducible SBZ. With the previous parameters, and fully relaxing the $3N$ atomic coordinates of the slab until all the $3N$ Cartesian force components are lower than 0.025 eV/\AA , the known structural and electronic properties of the clean Cu(110) surface can be accurately reproduced.^{73,74}

To find the stable adsorption geometry, the molecule has been located on different sites of the 2×2 cell for the two coverages $\theta=0.25 \text{ ML}$, corresponding to the $p(2 \times 2)$ structure (one molecule *per* 4 Cu surface atoms), and $\theta=0.50 \text{ ML}$, with a $c(2 \times 2)$ superstructure (two thiols *per* 4 Cu surface atoms). More than 10 different starting configuration for CH_3S and CH_3SH adsorption have been considered, varying the adsorption site (hollow H , longbridge L , shortbridge S , and top T), the angle between the normal to the surface and the S-C bond, and the hydrogen atoms orientation. The structure of the thiol-covered slab has been optimized, allowing the atomic coordinates of the adsorbed molecules and of the Cu slab to relax, until all the $3N$ Cartesian force components lower than 0.025 eV/\AA are obtained.

III. RESULTS

The DFT-GGA optimized bond lengths and angles of the isolated molecule CH_3SH are in good agreement with experimental data,⁷⁵ as shown in Fig. 1. The highest occupied molecular orbital (HOMO) and the lowest unoccupied molecular orbital (LUMO) wavefunctions of methanethiol are shown in Fig. 2: these states are, respectively, a p_z -MO completely localized on the S atom and an antibonding combination of p_x and p_y orbitals of S. The calculated HOMO-LUMO gap is of 4.5 eV. The orbital nature and energy levels of the MOs elucidate the origin of the hybridization among molecular orbitals and Cu states.

To investigate the physisorption of methanethiol on Cu(110), we analyze four different geometries with a starting S-surface distance of 1.2 \AA (see Fig. 3), namely (a) hollow site, with rotated hydrogen atoms (see Fig. 4), and the S-C axis normal to the surface, (b) hollow site, and S-C axis parallel to the surface, (c) long-bridge site, S-C axis normal

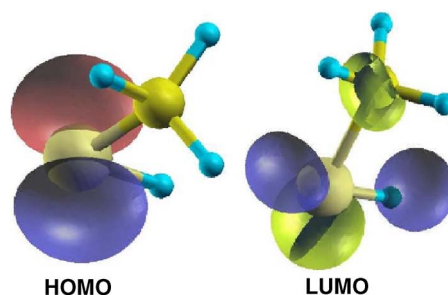


FIG. 2. (Color online) Methanethiol HOMO and LUMO charge distribution, for isovalues of $0.067e/\text{\AA}^3$ and $0.019e/\text{\AA}^3$, respectively.

to the surface, (d) short-bridge site, with the S-C axes normal to the surface. The DFT optimized geometries reported in Fig. 3 clearly show that the molecule remains almost unaffected by the presence of the surface. The final distance of the sulfur atom from the surface ranges from 1.94 \AA to 2.55 \AA . The binding energy E_b of adsorbed methanethiol is defined by

$$E_b = (E_{\text{sub}} + E_{\text{meth}}) - E_{\text{meth/sub}}, \quad (1)$$

where E_{sub} , E_{meth} , and $E_{\text{meth/sub}}$ are the total energy of the clean substrate, of the isolated methanethiol molecule, and of the $\text{CH}_3\text{SH}/\text{Cu}(110)$ system, respectively. Within this rule, attraction is denoted by positive binding energies while repulsion by negative ones. The binding energies for the reported configurations (see Fig. 3) are lower than 0.5 eV, as expected for molecule-metal interaction based on physisorption.

Larger binding energies are expected when the molecule dissociates, yielding H and CH_3S which chemisorbs, through sulfur, on Cu. For the methanethiolate, therefore, a wide study of adsorption configurations has been performed. For the $\text{CH}_3\text{S}/\text{Cu}(110)$ system, both $p(2 \times 2)$ and $c(2 \times 2)$ geometries have been analyzed: energies and structural parameters obtained for various adsorbate-surface configurations for the two coverages (all with an initial S-surface distance of

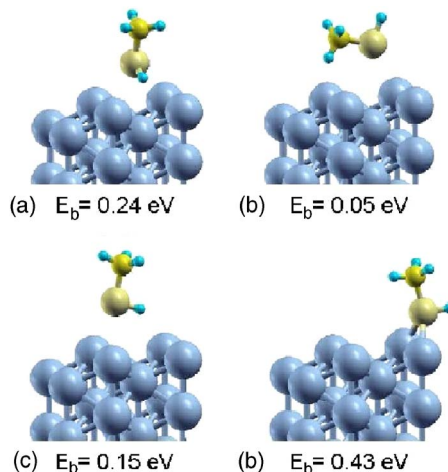


FIG. 3. (Color online) Physisorption geometries and binding energies (E_b) of methanethiol on Cu(110) (see text for details).

TABLE I. (Color online) Chemisorption geometries of methanethiolate on Cu(110), at $\theta=0.25$ ML coverage [$p(2 \times 2)$], from the least to the most stable. In the first column, starting geometry is identified by the adsorption site, the initial angle α between S-C bond and axes normal to the surface, the initial angle β (when defined) and the hydrogen atoms position. In the following columns, adsorption energy, Cu-S bond length, S-surface distance (h), the angles α and β , δ (see Fig. 4) and the relative variation of the surface unit cell dimensions with respect to the clean Cu surface (Δd_x , Δd_y , Δd_z) are reported. The last column shows the final relaxed geometry for the most stable configuration.

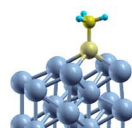
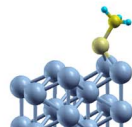
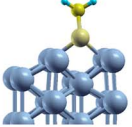
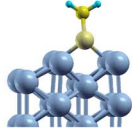
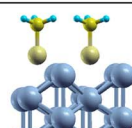
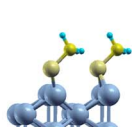
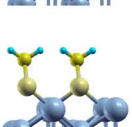
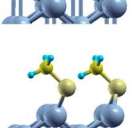
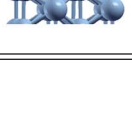
Initial geometry	E_b (eV)	$d_{\text{Cu-S}}$ (Å)	h (Å)	α	β	δ (Å)	Δd_x	Δd_y	Δd_z	geometry
$T/0^\circ$	0.588	2.19	1.81	55°	270°	1.15	0%	+2%	+5%	
$L/0^\circ$	0.855	2.29	1.35	0°		1.84	0%	0%	+6%	
$H/0^\circ$	1.034	2.48	1.27	0°		1.69	-1%	-8%	+28%	
$H/0^\circ(r)$	1.035	2.49	1.27	0°		1.69	-1%	-7%	+28%	
$H/45^\circ/90^\circ$	1.013	2.31	1.68	39°	90°	1.45	0%	-1%	+20%	
$H/90^\circ/90^\circ$	1.046	2.29	1.77	45°	90°	0.94	0%	-1%	+19%	
$L/0^\circ(r)$	1.026	2.37	1.36	45°	180°	1.75	-1%	-7%	+6%	
$H/90^\circ/270^\circ$	1.055	2.29	1.57	43°	270°	1.02	0%	-1%	+8%	
$S/0^\circ$	1.064	2.29	1.69	41°	270°	1.01	+1%	+8%	+8%	

TABLE II. (Color online) Chemisorption geometries of methanethiolate on Cu(110), at $\theta=0.50$ ML coverage [$c(2 \times 2)$], from the least to the most stable. Parameters reported are the same as of Table I.

Initial geometry	E_b (eV)	$d_{\text{Cu-S}}$ (Å)	h (Å)	α	β	δ (Å)	Δd_x	Δd_y	Δd_z	Relaxed geometry
$T/0^\circ$	0.817	2.30	1.34	0°		1.83	0%	0%	+13%	
$L/0^\circ$	0.818	3.43	1.35	0°		1.84	0%	-1%	+12%	
$H/0^\circ$	0.962	2.57	1.23	0°		1.83	0%	0%	+24%	
$H/0^\circ(r)$	0.965	2.56	1.23	0°		1.81	0%	0%	+23%	
$H/90^\circ/90^\circ$	1.126	2.27	1.73	51°	90°	0.66	-1%	0%	+13%	
$H/45^\circ/90^\circ$	1.133	2.26	1.60	54°	90°	0.52	+1%	0%	+13%	
$L/0^\circ(r)$	1.014	2.37	1.38	46°	180°	1.86	0%	-5%	+18%	
$H/90^\circ/270^\circ$	1.142	2.24	1.74	55°	270°	0.55	-1%	-1%	+13%	
$S/0^\circ$	1.144	2.26	1.76	56°	270°	0.53	+1%	+1%	+9%	

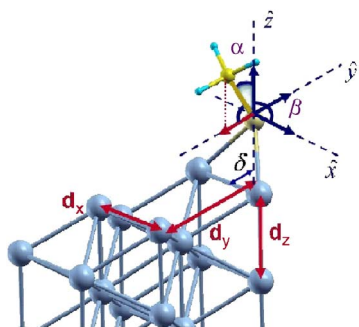


FIG. 4. (Color online) Geometrical parameters for a generic adsorption configuration: α is the angle formed by the S-C axes and the normal to the surface, β is the angle between the projection of the S-C axes on the surface plane and the x direction, d_x and d_y are the dimensions of the rectangular surface unit cell, d_z is the distance among the two outermost copper atomic planes and δ is the y shift from the nearest shortbridge site of the projection of the sulfur position on the surface. The geometry with hydrogen atoms rotated by 90° with respect to the configuration shown here, is called (r) in the following.

1.2 Å) are reported in Tables I and II where the corresponding relaxed geometries are also shown. The geometrical parameters used in Tables I and II are described in Fig. 4.

The binding energy E_b of adsorbed methanethiolate is calculated as

$$E_b = (E_{\text{sub}} + E_{\text{dimeth}}/2) - E_{\text{meth/sub}} \quad (2)$$

for $\theta=0.25$ ML, and

$$E_b = [(E_{\text{sub}} + E_{\text{dimeth}}) - E_{\text{meth/sub}}]/2 \quad (3)$$

for $\theta=0.50$ ML, where E_{sub} , E_{dimeth} , and $E_{\text{meth/sub}}$ are the total energy of the clean substrate, of the isolated dimethyl disulfide (CH_3S)₂ molecule, and of the $\text{CH}_3\text{S}/\text{Cu}(110)$ system, respectively.

The adsorption energies obtained for chemisorption configurations are in the range $E_b=0.59 \div 1.14$ eV, and the distance between S and metal surface in the range $h=1.23 \div 1.81$ Å, depending on the geometry. The Cu-S bond lengths for the most stable geometries are 2.29 Å and 2.26 Å for $p(2 \times 2)$ and $c(2 \times 2)$, respectively. The same stable configuration has been obtained starting from different initial geometries, in particular from the initial hollow adsorption site the molecule can move into the shortbridge one. Moreover, the differences in the E_b for various final configurations are quite small, for the 0.5 ML coverage the two shortbridge geometries (differing just for the hydrogen atoms rotation) and the longbridge one are quite close in energy (0.01 ÷ 0.03 eV). This shallow adsorption potential energy surface (PES) is quite similar to the results found for the adsorption of methanethiolate on Cu(111).⁵⁴ We note, finally, that the least stable configuration among the $p(2 \times 2)$ geometries is the one deriving from the top initial adsorption site. In this case, the sulfur bonds to just one Cu atom.

Concerning the relaxation of the Cu(110) surface resulting from exposure to methanethiolate, for the $p(2 \times 2)$ most favorable configuration, for which the effect is more intense than

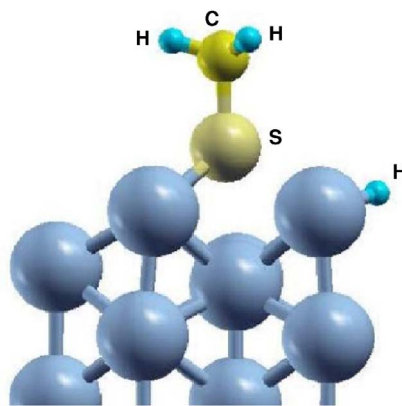


FIG. 5. (Color online) Lateral view of methanethiol dissociation into methanethiolate and hydrogen at the Cu(110) surface. The molecule is initially located in the hollow site, with the S-C axes normal to the surface. The corresponding adsorption energy is $E_b = 0.96$ eV.

for the $c(2 \times 2)$ geometry, we notice the presence of outwards relaxation of the outermost layer ($\sim 8\%$) with respect to the clean case, with associated corrugations (of height ~ 0.11 Å) and the formation of structures along the $[1\bar{1}0]$ direction, separated along the $[001]$ by ~ 7.5 Å: we can suppose that these sort of terraces can be reconduced to the valleys and the hills attested by STM images.⁵⁶

This analysis of structural properties uses the Generalized Gradient Approximation, which is known to give the most realistic values for bond lengths and energies^{68,70} of chemisorbed systems. LDA calculations, however, have been performed for the $p(2 \times 2)$ and $c(2 \times 2)$ most stable configurations, obtaining for E_b values larger by 17% for 0.25 ML and 34% for 0.5 ML, and smaller bond lengths (respectively, of 7% and of 2%) with respect to GGA results. This is in good agreement with previously reported theoretical results,⁶⁸ which assess the LDA overestimation of weak chemisorption (by $\approx 30\%$), and in general the best performances of GGA concerning energetic and structural properties of chemisorbed systems. In fact, apart from overestimating binding energy and underestimating bond lengths, LDA can also predict the wrong chemisorption site, as shown for the $\text{CO}/\text{Cu}(001)$ system.⁶⁸

IV. DISCUSSION

A. Structural analysis

Concerning physisorption, we can compare the physisorption energies (0.05 ÷ 0.43 eV) for the various considered configurations with the value for the ethanethiol physisorption on Au(111) (Ref. 32) of 0.32 eV. Also the distances from the surface are comparable for the two cases, being 2.22 Å (medium value) and 3.35 Å. We can suppose that, similarly to what has been calculated for methanethiol on Au(111), the adsorption process starts with a physisorbed state, with the methanethiol lying flat over the surface, and, after dissociation, methanethiolate chemisorbs with the S-C axis far from the parallel direction to the surface. We have directly ob-

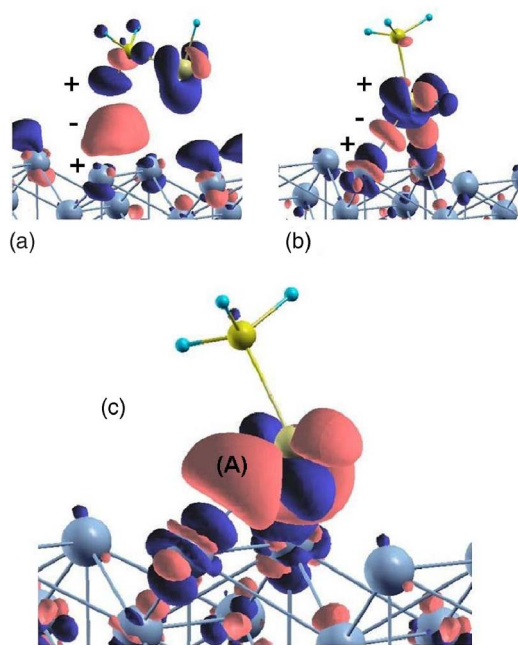


FIG. 6. (Color online) Charge-density differences, in the $p(2 \times 2)$ geometry, for (a) physisorption geometry with the CH_3SH lying flat on the $\text{Cu}(110)$, (b) physisorption geometry with the CH_3SH in the shortbridge site, normal to the surface, and (c) chemisorption state, shortbridge site. Regions of electron accumulation and depletion are displayed in red(−) and blue(+), respectively, for isosurface values of $\pm 0.0034e/\text{\AA}^3$ (a) and $\pm 0.0203e/\text{\AA}^3$ [(b) and (c)]. Charge distribution for the $c(2 \times 2)$ case is almost identical and not shown here.

served the decomposition (Fig. 5) of methanethiol in hydrogen and methanethiolate as expected from TPD results.⁵⁶

Concerning chemisorption, as clearly visible from the final relaxed geometries, starting both from hollow or shortbridge adsorption sites, the molecule of CH_3S aims to arrange itself with the S atom close to the shortbridge site and the S-C axes forming an angle of $40^\circ \div 50^\circ$ with respect to the normal to the surface. The adsorption site is shifted, with respect to the shortbridge site, toward the hollow site, by $\delta \approx 1.00 \text{ \AA}$ and $\delta \approx 0.54 \text{ \AA}$, for $p(2 \times 2)$ and $c(2 \times 2)$ respectively. This adsorption configuration is similar to the most stable geometry found for CH_3S on $\text{Au}(111)$.³² Moreover, the shortbridge site is slightly more favorable for $\beta = 270^\circ$ with respect to 90° . The S-Cu bond length in the most stable geometry is 2.26 \AA at 0.50 ML , and 2.29 \AA at 0.25 ML , to be compared with the value of 2.50 \AA obtained for $\text{CH}_3\text{S}/\text{Au}(111)$.³² The highest values of adsorption energy for both coverages are obtained for the initial configuration with the molecule located in the shortbridge site. Moreover, according to experimental results, $c(2 \times 2)$ superstructure is, for the most stable adsorption geometry, i.e., the slightly shifted shortbridge, energetically more favorable than the lower coverage $p(2 \times 2)$, with E_b for the single molecule higher by 7%. For other stable configurations, the $c(2 \times 2)$ coverage can yield a E_b higher by up to 28% with respect to the $p(2 \times 2)$ case. However it can be seen that, for less stable geometries, symmetry reasons do not allow molecules to dis-

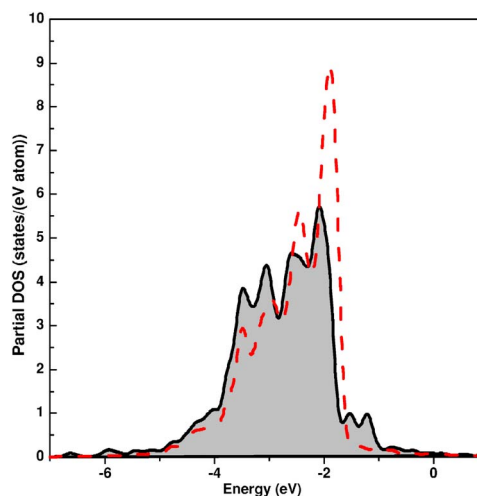


FIG. 7. (Color online) Partial d -PDOS/atom for the Cu surface layer of $\text{CH}_3\text{S}/\text{Cu}(110)$ (black solid line, light shaded) and d -PDOS/atom for the Cu surface layer of the clean surface (red dashed line).

pose themselves in the position of minimum energy and that, for a 0.5 ML coverage, the intermolecular repulsion implies a smaller E_b with respect to 0.25 ML .

B. Electronic analysis

We now turn to the analysis of the electronic properties for the most stable configurations found for both chemisorption and physisorption. We use, for this purpose, the density of states and the electronic charge density difference, defined as

$$\Delta\rho(\mathbf{r}) = \rho_{\text{meth/sub}}(\mathbf{r}) - \rho_{\text{sub}}(\mathbf{r}) - \rho_{\text{meth}}(\mathbf{r}), \quad (4)$$

where $\rho_{\text{meth/sub}}$, ρ_{sub} , and ρ_{meth} are the charge densities of the relaxed adsorbate-substrate system, of the clean relaxed surface, and of the molecule without substrate, respectively.

In Fig. 6(a) a physisorbed state [see Fig. 3(b)] is shown: the density changes due to regions of electronic accumulation (marked with −) and depletion (marked with +) illustrate the dipole formation, and the interaction between methanethiol and the metal substrate can be reconduced to electrostatic interaction rising from mutual polarization. In Fig. 6(b) the most stable adsorption configuration is reported for CH_3SH on $\text{Cu}(110)$, in the shortbridge site; this geometry has the largest binding energy (0.43 eV , see Fig. 3) among physisorption configurations (note the isosurface values range, more similar to the values of chemisorption). However, the charge distribution is more similar to the physisorption configuration, therefore we can consider this one as an intermediate state between physisorption and chemisorption, and a further confirmation that the shortbridge is the favorite adsorption site. Figure 6(c) shows, finally, the charge density difference for the most stable chemisorption state, at $\theta = 0.25 \text{ ML}$: electron accumulation [denoted by (A)] is clearly present among S atoms and the substrate.

To highlight the real nature of the bond, we study the

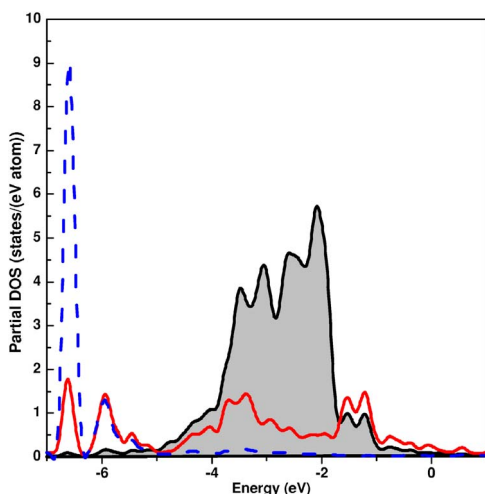


FIG. 8. (Color online) Partial d -PDOS/atom for the Cu surface layer of $\text{CH}_3\text{S}/\text{Cu}(110)$ (black solid line, light shaded), p -PDOS of sulfur (red solid line) and p -PDOS of carbon (blue dashed line).

differences between the density of states, resolved *per* atom and *per* angular momentum, in particular the modification induced on the d -PDOS of the Cu surface atoms by the CH_3S adsorption. Results are shown in Fig. 7 and Fig. 8. New states appear at the upper edge of the d -Cu band, at -1 eV, and the density of states increases at $-3 \div -4$ eV and decreases around -2 eV. Comparing this analysis with the density of states associated to sulfur and carbon atoms (see Fig. 8), we can attribute the observed variations in the copper properties to the presence of sulfur- p states (both at -1 eV and also at $-3 \div -4$ eV). Also two new peaks appear at -5.5 eV and -6.5 eV, associated to states completely localized on methanethiolate, both of sulfur-carbon p nature. Thanks to the Newns-Anderson model, and to previous results for similar systems,⁴⁵⁻⁴⁷ we can say that the state at -1 eV is of antibonding nature, while the states at $-3 \div -4$ eV have bonding character.

To further confirm these results, we calculate the spatial electronic charge density associated to the S-Cu hybrid states, shown in Fig. 9 and compare it with PDOS resolved by angular momentum components (not shown here). From the spatial shape of the hybrid states, it is possible to recognize the character of involved copper states and molecular orbitals. We find that both the HOMO of the molecule, of p_x nature in the slab geometry, and the sixth valence molecular orbital, of $p_y + p_z$ character in the same configuration, are involved in both bonding and antibonding states, hybridizing with various combinations of d -Cu states. In particular, in the antibonding region, all the states except the d_{xy} one are involved in the bond. We have identified different antibonding states: one of them, shown in [Fig. 9(a)], is located at $E_b = -1.30$ eV and is constituted by d_{yz} -Cu and $(p_x + p_y)$ -S orbitals. Two bonding states have also been found, at -2.83 eV and -3.55 eV, of $(d_{z^2} + d_{xy})$ -Cu/ $(p_x + p_y)$ -S, and d_{xz} -Cu/ p_y -S character, respectively. Hybrid states with energy smaller than -5.82 eV are derived from the other valence molecular orbitals.

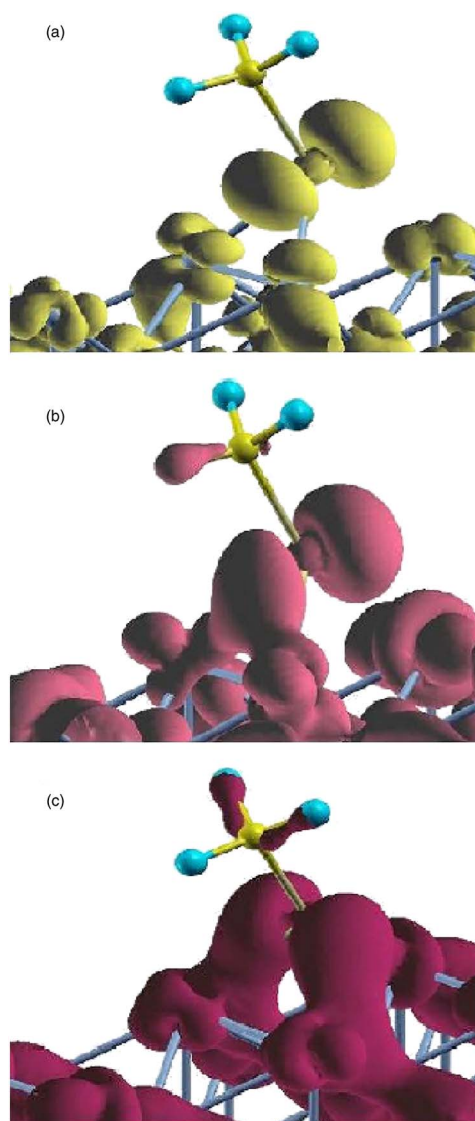


FIG. 9. (Color online) Spatial electronic charge density (squared Kohn-Sham orbital) at the Γ point, of the antibonding (a) and bonding [(b) and (c)] sulfur-copper states, for isovalues of $6.8 \times 10^{-3} e/\text{\AA}^3$, $2.0 \times 10^{-3} e/\text{\AA}^3$, and $1.7 \times 10^{-3} e/\text{\AA}^3$, respectively. The bonding or antibonding character is clearly visible in the electronic charge distribution.

V. CONCLUSIONS

In this paper we have presented the structural and the electronic properties of a simple thiol chemisorbed on Cu(110), using *ab initio* methods. The difficulty of the analysis resides in the lack of clear and definitive experimental structural data. However, we are able to identify the most stable adsorption site and the corresponding molecular geometry. The 0.5 ML coverage gives the highest methanethiolate binding energy, confirming the observed stability of the $c(2 \times 2)$ phase.⁵⁶ We also can exclude that the methanethiolate adsorbs in a lying-down configuration, as proposed by Ref. 58. As expected, the determination of geometry adsorption is not straightforward due to the low energy differences between various configurations.

The structural and electronic analysis has revealed that the main methanethiol-surface interactions come from the mixing of p orbitals of the molecule with d states of the surface Cu atoms, in this way confirming the importance of S in the chemisorption of such kind of organic adsorbate on Cu(110).⁷⁶

ACKNOWLEDGMENTS

The authors acknowledge the SPACI consortium for providing computational facilities. One of the authors (L.C.) acknowledges the support by the European Project SA-NANO (Contract No. STRP013698).

- ¹R. G. Nuzzo and D. L. Allara, *J. Am. Chem. Soc.* **105**, 4481 (1983).
- ²M. Gomez, J. Li, and A. E. Kaifer, *Langmuir* **7**, 1797 (1991).
- ³O. Chailapakul and R. M. Crooks, *Langmuir* **9**, 884 (1993).
- ⁴W. G. Schmidt and K. Seino, *Surf. Rev. Lett.* **10**, 221 (2003).
- ⁵A. Ulman, *Chem. Rev. (Washington, D.C.)* **96**, 1533 (1996).
- ⁶A. Ulman, *An Introduction to Ultrathin Organic Films: Langmuir Blodgett to Self-Assembly* (Academic, Boston, 1991).
- ⁷G. M. Whitesides, J. P. Manthias, and C. T. Seto, *Science* **254**, 1312 (1991).
- ⁸L. H. Dubois and R. G. Nuzzo, *Annu. Rev. Phys. Chem.* **43**, 437 (1992).
- ⁹A. W. Adamson, *Physical Chemistry of Surfaces*, 3rd ed. (Wiley, New York, 1976).
- ¹⁰V. Perebeinos and M. Newton, *Chem. Phys.* **319**, 159 (2005).
- ¹¹C. N. Sayre and D. M. Collard, *Langmuir* **4**, 714 (1997).
- ¹²J. A. M. Sondag-Huethorst, C. Schonenberger, and L. G. L. Fokink, *J. Phys. Chem.* **98**, 6826 (1994).
- ¹³H. Wolf, H. Ringsdorf, E. Delamarche, T. Takami, H. Kang, B. Michel, C. Gerber, M. Jaschke, H.-J. Butt, and E. Bamberg, *J. Phys. Chem.* **99**, 7102 (1995).
- ¹⁴P. Fenter, A. Eberhardt, and P. Eisenberg, *Science* **266**, 1216 (1994).
- ¹⁵S. E. Creager, L. A. Hockett, and G. K. Rowe, *Langmuir* **8**, 854 (1992).
- ¹⁶L. Sun and R. M. Crooks, *Langmuir* **9**, 1951 (1993).
- ¹⁷E. Delamarche, B. Michel, H. Kang, and C. Gerber, *Langmuir* **10**, 4103 (1994).
- ¹⁸J. P. Bucher, L. Santesson, and K. Kern, *Langmuir* **10**, 979 (1994).
- ¹⁹L. Strong and G. M. Whitesides, *Langmuir* **4**, 546 (1988).
- ²⁰N. Camillone III, P. Eisenberg, T. Y. B. Leung, P. Schwartz, G. Scoles, G. E. Poirier, and M. J. Tarlov, *J. Chem. Phys.* **101**, 11031 (1994).
- ²¹C. E. D. Chidsey, G. Y. Liu, G. Scoles, and J. Wang, *Langmuir* **6**, 1804 (1990).
- ²²P. Fenter, P. Eisenberg, J. Li, N. Camillone III, S. Bernasek, G. Scoles, T. A. Ramanarayanan, and K. S. Liang, *Langmuir* **7**, 2013 (1991).
- ²³M. D. Porter, T. B. Bright, D. L. Allara, and C. E. D. Chidsey, *J. Am. Chem. Soc.* **109**, 3559 (1987).
- ²⁴M. M. Walczak, C. Chung, S. M. Stol, C. A. Widrig, and M. D. Porter, *J. Am. Chem. Soc.* **113**, 2370 (1991).
- ²⁵P. E. Laibinis, G. M. Whitesides, D. L. Allara, T. Y.-T., A. N. Parikh, and R. G. Nuzzo, *J. Am. Chem. Soc.* **113**, 7152 (1991).
- ²⁶M. Scheffler and C. Stampfl, "Theory of Adsorption on Metal Substrates," in *Handbook of Surface Science, Vol. 2: Electronic Structure*, edited by K. Horn and M. Scheffler (Elsevier, Amsterdam, 2000), pp. 286–356.
- ²⁷H. Sellers, A. Ulman, Y. Shnidman, and J. Eilers, *J. Am. Chem. Soc.* **115**, 9389 (1993).
- ²⁸D. Kruger, H. Fuchs, R. Rousseau, D. Marx, and M. Parrinello, *J. Chem. Phys.* **115**, 4776 (2001).
- ²⁹L. M. Molina and B. Hammer, *Chem. Phys. Lett.* **320**, 264 (2002).
- ³⁰P. Maksymovych, D. C. Sorescu, and J. T. Yates, *Phys. Rev. Lett.* **97**, 146103 (2006).
- ³¹R. Mazzarello, A. Cossaro, A. Verdini, R. Rousseau, L. Casalis, M. F. Danisman, L. Floreano, S. Scandolo, A. Morgante, and G. Scoles, *Phys. Rev. Lett.* **98**, 016102 (2007).
- ³²Y. Yourdshahyan and A. M. Rappe, *J. Chem. Phys.* **117**, 825 (2002).
- ³³M. C. Vargas, P. Giannozzi, A. Selloni, and G. Scoles, *J. Phys. Chem. B* **105**, 9509 (2001).
- ³⁴H. Gronbeck, A. Curioni, and W. Andreoni, *J. Am. Chem. Soc.* **122**, 3839 (2000).
- ³⁵W. Andreoni, A. Curioni, and H. Gronbeck, *Int. J. Quantum Chem.* **80**, 598 (2000).
- ³⁶Y. Yourdshahyan, H. K. Zhang, and A. M. Rappe, *Phys. Rev. B* **63**, 081405(R) (2001).
- ³⁷R. Di Felice, A. Selloni, and E. Molinari, *J. Phys. Chem. B* **107**, 1151 (2003).
- ³⁸A. Kuhnle, T. Linderoth, B. Hammer, and F. Besenbacher, *Nature (London)* **415**, 891 (2002).
- ³⁹H. Orita and N. Itoh, *Surf. Sci.* **550**, 177 (2004).
- ⁴⁰V. De Renzi, R. Rousseau, D. Marchetto, R. Biagi, S. Scandolo, and U. del Pennino, *Phys. Rev. Lett.* **95**, 046804 (2005).
- ⁴¹G. Heimel, L. Romaner, J.-L. Brédas, and E. Zojer, *Phys. Rev. Lett.* **96**, 196806 (2006).
- ⁴²M. E. Castro, S. Ahkter, A. Golchet, and J. M. White, *Langmuir* **7**, 126 (1991), and references therein.
- ⁴³D. R. Mullins and P. F. Lyman, *J. Phys. Chem.* **97**, 9226 (1993).
- ⁴⁴J. K. Norskov and B. Hammer, in *Chemisorption and Reactivity of Supported Clusters and Thin Films*, edited by R. M. Lambert and G. Pacchioni (Kluwer Academic, Dordrecht, 1997).
- ⁴⁵L. Chiodo and P. Monachesi, *Phys. Rev. B* **75**, 075404 (2007).
- ⁴⁶P. Monachesi, L. Chiodo, and R. Del Sole, *Phys. Rev. B* **69**, 165404 (2004).
- ⁴⁷A. Ferretti and R. Di Felice, *Phys. Rev. B* **70**, 115412 (2004).
- ⁴⁸A. Marini, G. Onida, and R. Del Sole, *Phys. Rev. B* **64**, 195125 (2001).
- ⁴⁹C. Baldacchini, L. Chiodo, F. Allegretti, C. Mariani, M. G. Betti, P. Monachesi, and R. Del Sole, *Phys. Rev. B* **68**, 195109 (2003).
- ⁵⁰L. Gross, F. Moresco, M. Alemani, T. Hao, A. Gourdon, C. Joachim, and K. H. Rieder, *Chem. Phys. Lett.* **371**, 750 (2003).
- ⁵¹F. Bussolotti, M. G. Betti, and C. Mariani, *Phys. Rev. B* **74**, 125422 (2006).
- ⁵²C. Mariani, F. Allegretti, V. Corradini, G. Contini, V. Di Castro,

- C. Baldacchini, and M. G. Betti, Phys. Rev. B **66**, 115407 (2002).
- ⁵³L. Chiodo and P. Monachesi (unpublished).
- ⁵⁴M. Konopka, R. Rousseau, I. Stich, and D. Marx, Phys. Rev. Lett. **95**, 096102 (2005).
- ⁵⁵H. Kondoh, N. Saito, F. Matsui, T. Yokoyama, T. Ohta, and H. Kuroda, J. Phys. Chem. **105**, 12870 (2001).
- ⁵⁶A. F. Carley, P. R. Davies, R. V. Jones, K. R. Harikumar, M. Wyn Roberts, and C. J. Welsby, Top. Catal. **22**, 161 (2003).
- ⁵⁷A. F. Carley, P. R. Davies, R. V. Jones, K. R. Harikumar, G. U. Kulkarni, and M. W. Roberts, Surf. Sci. **447**, 39 (2000).
- ⁵⁸J. G. Lee and J. T. Yates, J. Phys. Chem. B **107**, 10540 (2003).
- ⁵⁹A. Kühnle, S. Vollmer, T. R. Linderoth, G. Witte, C. Wöll, and F. Besenbacher, Langmuir **18**, 5558 (2002), and references therein.
- ⁶⁰D. Martin (private communication).
- ⁶¹R. Dreizler and E. Gross, *Density Functional Theory* (Plenum Press, New York, 1995).
- ⁶²J. P. Perdew, K. Burke, and M. Ernzerhof, Phys. Rev. Lett. **77**, 3865 (1996).
- ⁶³J. P. Perdew and A. Zunger, Phys. Rev. B **23**, 5048 (1981).
- ⁶⁴S. Baroni, A. Dal Corso, S. de Gironcoli, and P. Giannozzi, www.pwscf.org/
- ⁶⁵A. Kokalj, Comput. Mater. Sci. **28**, 155 (2003). Code available from <http://www.xcrysden.org/>
- ⁶⁶M. C. Payne, M. P. Teter, D. Allan, T. A. Arias, and J. D. Joannopoulos, Rev. Mod. Phys. **64**, 1045 (1992).
- ⁶⁷N. W. Ashcroft and N. D. Mermin, *Solid State Physics* (Saunders, Philadelphia, 1976).
- ⁶⁸F. Favot, A. Dal Corso, and A. Baldereschi, J. Chem. Phys. **114**, 483 (2001).
- ⁶⁹M. Methfessel and A. T. Paxton, Phys. Rev. B **40**, 3616 (1989).
- ⁷⁰R. A. Bartynski and T. Gustafsson, Phys. Rev. B **33**, 6588 (1986).
- ⁷¹P. Monachesi, M. Palummo, R. Del Sole, R. Ahuja, and O. Eriksson, Phys. Rev. B **64**, 115421 (2001).
- ⁷²C. J. Fall, N. Binggeli, and A. Baldereschi, Phys. Rev. B **61**, 8489 (2000).
- ⁷³P. Monachesi, M. Palummo, R. Del Sole, A. Grechnev, and O. Eriksson, Phys. Rev. B **68**, 035426 (2003).
- ⁷⁴<http://www.fhi-berlin.mpg.de/th/fhi98md/doc/main/node15.html>
- ⁷⁵Available online at <http://webbook.nist.gov/cgi/cbook.cgi?Name=methanethiolUnits=SI>
- ⁷⁶J.-G. Lee, J. Lee, and J. T. Yates, Jr., J. Phys. Chem. B **108**, 1686 (2004).